A Numerical Model for Three-Phase Liquid–Vapor–Gas Flows with Relaxation Processes

Tore Flåtten, Marica Pelanti and Keh-Ming Shyue

Abstract We are interested in three-phase flows involving the liquid and vapor phases of one species and a third inert gaseous phase. We describe these flows by a single-velocity multiphase flow model composed of the phasic mass and total energy equations, the volume fraction equations, and the mixture momentum equation. The model includes stiff mechanical and thermal relaxation source terms for all the phases and chemical relaxation terms to describe mass transfer between the liquid and vapor phases of the species that may undergo transition. The homogeneous hyperbolic portion of the equations is solved numerically via a finite volume wave propagation scheme. Relaxation terms are treated by routines that exploit algebraic equilibrium conditions for the relaxed states. We present numerical results for a three-phase cavitation tube test, showing that the predicted wave speed for different levels of activation of instantaneous relaxation processes agrees with the theoretical findings on the sub-characteristic interlacing of the wave speeds of the corresponding hierarchy of relaxed models. A two-dimensional simulation of an underwater explosion is also presented.

Keywords Multiphase compressible flows · Relaxation processes
Phase transition · Finite volume schemes · Riemann solvers

Mathematics Subject Classification 65M08 · 76T10

T. Flåtten
Norwegian University of Science and Technology, Kolbjørn Hejes vei 2, 7491 Trondheim, Norway
e-mail: toref@math.uio.no

M. Pelanti (✉)
IMSIA, UMR 9219 ENSTA ParisTech - EDF - CNRS - CEA, Université Paris-Saclay, 828 Boulevard des Maréchaux,91762 Palaiseau Cedex, France
e-mail: marica.pelanti@ensta-paristech.fr

K.-M. Shyue
Department of Mathematics, National Taiwan University,Taipei 106, Taiwan
e-mail: shyue@ntu.edu.tw

C. Klingenberg and M. Westdickenberg (eds.), *Theory, Numerics and Applications of Hyperbolic Problems II*, Springer Proceedings in Mathematics & Statistics 237, https://doi.org/10.1007/978-3-319-91548-7_32

1 Introduction

We are interested in the simulation of three-phase flows involving the liquid and vapor phases of one species and a third non-condensable gaseous phase. Applications are, for instance, the simulation of flows around high speed cavitating underwater devices [13] and the modeling of underwater explosions [2, 15]. We describe these multiphase flows by a hyperbolic single-velocity compressible flow model with stiff pressure relaxation, which extends the two-phase formulation that we have considered in previous work [11]. The model includes thermal relaxation terms to account for heat transfer processes between all the phases and chemical relaxation terms to describe mass transfer between the liquid and vapor phases of the species that may undergo transition. Similar multiphase models have been, for instance, presented in [7, 13]. The formulation that we adopt here with phasic total energy equations is particularly convenient to develop a *mixture-energy-consistent* numerical model, in the sense defined in [11] for the two-phase case (see also Sect. 3). The homogeneous hyperbolic portion of the equations is solved numerically via a finite volume wave propagation scheme that uses a simple HLLC-type Riemann solver. Stiff relaxation source terms are handled by efficient numerical procedures that exploit algebraic equilibrium conditions for the relaxed states. One special focus of this work is the study of the effects of heat and mass transfer on the speed of wave propagation. We first derive analytical expressions of the speed of sound of the relaxed multiphase models associated with the different levels of activation of infinitely fast relaxation processes, and we demonstrate that sub-characteristic conditions hold. We then show through a one-dimensional three-phase cavitation tube experiment that the behavior of the wave speed predicted numerically is consistent with our theoretical findings. This paper is organized as follows. In Sect. 2, we present the multiphase flow model under study. Here we also analyze the characteristic speeds of the relaxed models associated with the parent relaxation model. In Sect. 3, we illustrate the numerical method that we have developed to solve the three-phase flow equations. Some numerical experiments are finally presented in Sect. 4, including a two-dimensional simulation of an underwater explosion.

2 Single-Velocity Multiphase Compressible Flow Model

We consider an inviscid compressible flow composed of N phases that we assume in kinematic equilibrium with velocity $\mathbf{u}$. In this work, we are specifically interested in three-phase flows, $N = 3$; nonetheless, we shall present here a general multiphase flow formulation. The volume fraction, density, internal energy per unit volume, and pressure of each phase will be denoted by α_k, ρ_k, $\mathcal{E}_k$, p_k, $k = 1, \ldots N$, respectively. We will denote the total energy for the kth phase with $E_k = \mathcal{E}_k + \rho_k \frac{|\mathbf{u}|^2}{2}$. The saturation condition is $\sum_{k=1}^{N} \alpha_k = 1$. The mixture density is $\rho = \sum_{k=1}^{N} \alpha_k \rho_k$, the mixture internal energy is $\mathcal{E} = \sum_{k=1}^{N} \alpha_k \mathcal{E}_k$, and the mixture total energy is

$E=\sum_{k=1}^{N}\alpha_k E_k=\mathcal{E}+\rho\frac{|\mathbf{u}|^2}{2}$. Mechanical and thermal transfer processes are considered in general for all the phases. We assume that one species in the mixture can undergo phase transition, so that it can exist as a vapor or a liquid phase, and mass transfer terms are accounted for this species only. We will use the subscripts 1 and 2 to denote the liquid and vapor phases of this species. We describe the N-phase flow under consideration by a compressible flow model that extends the six-equation two-phase flow system that we studied in [11]. The model system is composed of the volume fraction equations for $N-1$ phases, the mass and total energy equations for all the N phases, and d mixture momentum equations, where d denotes the spatial dimension:

$$\partial_t\alpha_k+\mathbf{u}\cdot\nabla\alpha_k=\sum_{j=1}^{N}\mathcal{P}_{kj}\,,\quad k=1,3,\dots,N, \tag{1a}$$

$$\partial_t(\alpha_1\rho_1)+\nabla\cdot(\alpha_1\rho_1\mathbf{u})=\mathcal{M}, \tag{1b}$$

$$\partial_t(\alpha_2\rho_2)+\nabla\cdot(\alpha_2\rho_2\mathbf{u})=-\mathcal{M} \tag{1c}$$

$$\partial_t(\alpha_k\rho_k)+\nabla\cdot(\alpha_k\rho_k\mathbf{u})=0\,,\quad k=3,\dots,N\,, \tag{1d}$$

$$\partial_t(\rho\mathbf{u})+\nabla\cdot\left(\rho\mathbf{u}\otimes\mathbf{u}+\left(\sum_{k=1}^{N}\alpha_k p_k\right)\mathbb{I}\right)=0\,, \tag{1e}$$

$$\partial_t(\alpha_1E_1)+\nabla\cdot(\alpha_1(E_1+p_1)\mathbf{u})+\Upsilon_1=-\sum_{j=1}^{N}p_{\mathrm{I}1j}\mathcal{P}_{1j}+\sum_{j=1}^{N}\mathcal{Q}_{1j}+\left(g_{\mathrm{I}}+\frac{|\mathbf{u}|^2}{2}\right)\mathcal{M}, \tag{1f}$$

$$\partial_t(\alpha_2E_2)+\nabla\cdot(\alpha_2(E_2+p_2)\mathbf{u})+\Upsilon_2=-\sum_{j=1}^{N}p_{\mathrm{I}2j}\mathcal{P}_{2j}+\sum_{j=1}^{N}\mathcal{Q}_{2j}-\left(g_{\mathrm{I}}+\frac{|\mathbf{u}|^2}{2}\right)\mathcal{M}, \tag{1g}$$

$$\partial_t(\alpha_kE_k)+\nabla\cdot(\alpha_k(E_k+p_k)\mathbf{u})+\Upsilon_k=-\sum_{j=1}^{N}p_{\mathrm{I}kj}\mathcal{P}_{kj}+\sum_{j=1}^{N}\mathcal{Q}_{kj}\,,\quad k=3,\dots,N\,. \tag{1h}$$

The non-conservative terms Υ_k appearing in the phasic total energy Eqs. (1f)–(1h) are given by

$$\Upsilon_k=\mathbf{u}\cdot\left(Y_k\nabla\left(\sum_{j=1}^{N}\alpha_j p_j\right)-\nabla(\alpha_k p_k)\right)\,,\quad k=1,\dots,N\,, \tag{1i}$$

where $Y_k=\frac{\alpha_k\rho_k}{\rho}$ denotes the mass fraction of phase k. In the system above, $\mathcal{P}_{kj}$ and $\mathcal{Q}_{kj}$ represent the volume transfer and the heat transfer, respectively, between the phases k and j, $k,j=1,\dots N$. The term $\mathcal{M}$ indicates the mass transfer between the liquid and vapor phases indexed with 1 and 2. The transfer terms are defined as relaxation terms:

$$\mathcal{P}_{kj}=\mu_{kj}(p_k-p_j)\,,\quad \mathcal{Q}_{kj}=\vartheta_{kj}(T_j-T_k)\,,\quad \mathcal{M}=\nu(g_2-g_1)\,, \tag{2}$$

where T_k denotes the phasic temperature, g_k the phasic chemical potential, and where we have introduced the mechanical, thermal, and chemical relaxation parameters $\mu_{kj}=\mu_{jk}\geq 0$, $\vartheta_{kj}=\vartheta_{jk}\geq 0$, and $\nu=\nu_{12}=\nu_{21}\geq 0$, respectively. Note that $\mathcal{P}_{kj}=-\mathcal{P}_{jk}$ and $\mathcal{Q}_{kj}=-\mathcal{Q}_{jk}$. The quantities $p_{\mathrm{I}kj}=p_{\mathrm{I}jk}$ are interface pressures and g_{I} is an interface chemical potential. We shall assume that mechanical equilibrium is reached instantaneously for all the phases, $\mu_{kj}=\mu_{jk}\equiv\mu\to+\infty$; that is, mechanical relaxation processes are infinitely fast. Following [14], we then consider that thermal and chemical relaxation processes are either inactive, $\vartheta_{kj} = 0$, $\nu = 0$, or they act infinitely fast, $\vartheta_{kj} \to +\infty$, $\nu \to +\infty$. Heat and mass transfer may be activated at selected locations, for instance, at interfaces for a phase pair (k, j), identified by $\min(\alpha_k, \alpha_j) > \epsilon$, where ϵ is a tolerance.

The closure of the system (1) is obtained through the specification of an equation of state (EOS) for each phase $p_k = p_k(\mathcal{E}_k, \rho_k)$, $T_k = T_k(p_k, \rho_k)$. Here in particular we will adopt the widely used stiffened gas (SG) equation of state:

$$p_k(\mathcal{E}_k, \rho_k) = (\gamma_k - 1)\mathcal{E}_k - \gamma_k \varpi_k - (\gamma_k - 1)\eta_k \rho_k \quad \text{and} \quad T_k(p_k, \rho_k) = \frac{p_k + \varpi_k}{\kappa_{vk}\rho_k(\gamma_k - 1)}, \tag{3}$$

where γ_k, ϖ_k, η_k, and κ_{vk} are constant material-dependent parameters. The corresponding expression for the phasic entropy is $s_k = \kappa_{vk} \log(T_k^{\gamma_k}(p_k + \varpi_k)^{-(\gamma_k - 1)}) + \eta'_k$, where η'_k = constant, and $g_k = h_k - T_k s_k$. The parameters for the SG EOS for the liquid and vapor phases of the species that may undergo transition are determined by imposing that the theoretical saturation curve defined by $g_1 = g_2$ matches the experimental one for the considered material [6]. The mixture pressure law is determined by the mixture energy relation $\mathcal{E} = \sum_{k=1}^{N} \alpha_k \mathcal{E}_k(p, \rho_k)$, where we have used the mechanical equilibrium conditions $p_k = p$, $\forall k = 1, \ldots, N$ in the phasic energy laws $\mathcal{E}_k(p_k, \rho_k)$.

Since here we will consider relaxation parameters either $= 0$ or $\to \infty$, a specification of the expression for the interface quantities $p_{\mathrm{I}kj}$, g_{I} is not needed. Nevertheless, let us remark that the definition of these interface quantities must be consistent with the second law of thermodynamics, which requires a nonnegative entropy production for the mixture. By writing the equation for the mixture entropy and by following the arguments in [3], one can infer the following sufficient consistency conditions: $p_{\mathrm{I}kj} \in [\min(p_k, p_j), \max(p_k, p_j)]$, and $g_{\mathrm{I}} \in [\min(g_1, g_2), \max(g_1, g_2)]$.

The model (1) is hyperbolic, and the associated speed of sound c_{f} (non-equilibrium or frozen sound speed) is

$$c_{\mathrm{f}} = \sqrt{\sum_{k=1}^{N} Y_k c_k^2}\,, \tag{4}$$

where c_k is the speed of sound of phase k, which can be expressed as $c_k = \sqrt{\Gamma_k h_k + \chi_k}$, where $h_k = (\mathcal{E}_k + p_k)/\rho_k$ is the specific enthalpy of phase k, $\Gamma_k = (\partial p_k / \partial \mathcal{E}_k)_{\rho_k}$, and $\chi_k = (\partial p_k / \partial \rho_k)_{\mathcal{E}_k}$.

2.1 Hierarchy of Multiphase Relaxed Models and Speed of Sound

In the considered limit of instantaneous mechanical relaxation $\mu_{kj} \equiv \mu \to \infty$, the model system (1) reduces to a hyperbolic single-velocity single-pressure model which is a generalization of the five-equation two-phase flow model of Kapila et al. [5]. The reduced pressure equilibrium model can be derived by means of asymptotic techniques. Denoting with p the equilibrium pressure, we obtain the following relaxed system, composed of $2N + d$ equations:

$$\partial_t\alpha_1 + \mathbf{u}\cdot\nabla\alpha_1 = K_1\nabla\cdot\mathbf{u} + \tfrac{\Gamma_1}{\rho_1 c_1^2}\sum_{j=2}^{N} Q_{1j} - \alpha_1\tfrac{\rho c_p^2}{\rho_1 c_1^2}\sum_{\substack{j,i=1\\ i>j}}^{N} Q_{ji}\left(\tfrac{\Gamma_j}{\rho_j c_j^2} - \tfrac{\Gamma_i}{\rho_i c_i^2}\right)$$

$$+\,\tfrac{\rho c_p^2}{\rho_1 c_1^2}\left((\Gamma_1(g_{\mathrm{I}} - h_1) + c_1^2)\sum_{\substack{j=1\\ j\neq k}}^{N}\tfrac{\alpha_j}{\rho_j c_j^2} + (\Gamma_2(g_{\mathrm{I}} - h_2) + c_2^2)\tfrac{\alpha_1}{\rho_2 c_2^2}\right)\mathcal{M}, \tag{5a}$$

$$\partial_t\alpha_k + \mathbf{u}\cdot\nabla\alpha_k = K_k\nabla\cdot\mathbf{u} + \tfrac{\Gamma_k}{\rho_k c_k^2}\sum_{\substack{j=1\\ j\neq k}}^{N} Q_{kj} - \alpha_k\tfrac{\rho c_p^2}{\rho_k c_k^2}\sum_{\substack{j,i=1\\ i>j}}^{N} Q_{ji}\left(\tfrac{\Gamma_j}{\rho_j c_j^2} - \tfrac{\Gamma_i}{\rho_i c_i^2}\right)$$

$$+\,\rho c_p^2\tfrac{\alpha_k}{\rho_k c_k^2}\left(\tfrac{\Gamma_2(g_{\mathrm{I}}-h_2)+c_2^2}{\rho_2 c_2^2} - \tfrac{\Gamma_1(g_{\mathrm{I}}-h_1)+c_1^2}{\rho_1 c_1^2}\right)\mathcal{M}, \quad k = 3,\ldots,N\,, \tag{5b}$$

$$\partial_t(\alpha_1\rho_1) + \nabla\cdot(\alpha_1\rho_1\mathbf{u}) = \mathcal{M}\,, \tag{5c}$$

$$\partial_t(\alpha_2\rho_2) + \nabla\cdot(\alpha_2\rho_2\mathbf{u}) = -\mathcal{M}\,, \tag{5d}$$

$$\partial_t(\alpha_k\rho_k) + \nabla\cdot(\alpha_k\rho_k\mathbf{u}) = 0\,, \quad k = 3,\ldots,N\,, \tag{5e}$$

$$\partial_t(\rho\mathbf{u}) + \nabla\cdot(\rho\mathbf{u}\otimes\mathbf{u} + p\mathbb{I}) = 0\,, \tag{5f}$$

$$\partial_t E + \nabla\cdot((E + p)\mathbf{u}) = 0\,, \tag{5g}$$

where

$$K_k = \rho c_p^2\alpha_k\sum_{\substack{j=1\\ j\neq k}}^{N}\alpha_j\left(\tfrac{1}{\rho_k c_k^2} - \tfrac{1}{\rho_j c_j^2}\right) = \alpha_k\left(\tfrac{\rho c_p^2}{\rho_k c_k^2} - 1\right)\,. \tag{6}$$

In the relations above, we have introduced the pressure equilibrium speed of sound c_p (a generalization of Wood's sound speed), defined by

$$c_p = \left(\rho\sum_{k=1}^{N}\frac{\alpha_k}{\rho_k c_k^2}\right)^{-\frac{1}{2}}\,. \tag{7}$$

Let us note that the source terms in the volume fraction Eqs. (5a), (5b) result from the asymptotic limit of instantaneous pressure relaxation.

More generally, a hierarchy of hyperbolic multiphase flow models can be established based on the assumptions on equilibria attained by different combinations of instantaneous relaxation processes. In particular, we study here the expression of the speed of sound for the relaxed models in the hierarchy, similar to [3, 4]. We can derive the following results, valid for any equation of state, whose full demonstration will be detailed elsewhere, together with the derivation of (5). First, assuming instantaneous mechanical equilibrium $\mu_{jk} \equiv \mu \to +\infty$ for all the phases and thermal equilibrium $\vartheta_{kj} \equiv \vartheta \to +\infty$ for M phases, $2 \le M \le N$, we obtain a hyperbolic relaxed system of $2N - M + 1 + d$ equations characterized by the speed of sound $c_{pT,M}$, defined by

$$\frac{1}{{c_{pT,M}}^2} = \frac{1}{{c_p}^2} + \frac{\rho T}{\sum_{k=1}^{M} C_{pk}}\sum_{k=1}^{M-1} C_{pk}\sum_{j=k+1}^{M} C_{pj}\left(\frac{\Gamma_j}{\rho_j c_j^2} - \frac{\Gamma_k}{\rho_k c_k^2}\right)^2\,, \tag{8}$$

where T denotes the equilibrium temperature, $C_{pk} = \alpha_k \rho_k \kappa_{pk}$, $\kappa_{pk} = (\partial h_k / \partial T_k)_{p_k}$ (specific heat at constant pressure), and we recall $\Gamma_k = (\partial p_k / \partial \mathcal{E}_k)_{\rho_k}$. If additionally we assume instantaneous chemical relaxation between the liquid and vapor phases 1 and 2, $\nu \to +\infty$, we obtain a hyperbolic relaxed system of $2(N - M + 1) + d$ equations characterized by a speed of sound $c_{pTg,M}$, defined by

$$\frac{1}{{c_{pTg,M}}^2} = \frac{1}{{c_{pT,M}}^2} + \frac{\rho T}{\sum_{k=1}^{M} C_{pk}} \left(\sum_{k=1}^{M} \frac{\Gamma_k C_{pk}}{\rho_k c_k^2} - \frac{1}{T} \left(\frac{\mathrm{d}T}{\mathrm{d}p} \right)_{\text{sat}} \sum_{k=1}^{M} C_{pk} \right)^2 , \tag{9}$$

where we have introduced the derivatives $(\mathrm{d}T/\mathrm{d}p)_{\text{sat}}$ evaluated on the liquid–vapor saturation curve. Analogously to the two-phase case [3], it is easy to observe that subcharacteristic conditions hold; namely, the speed of sound of the N-phase mixture is reduced whenever an additional equilibrium assumption is introduced: $c_{pTg} \equiv c_{pTg,N} \le c_{pTg,M}$, $c_{pT} \equiv c_{pT,N} \le c_{pT,M}$, and $c_{pTg} < c_{pT} < c_p < c_{\mathrm{f}}$.

Remark. In [11], an additional term of the form $\mathcal{M}/\rho_{\mathrm{I}}$ was written in the volume fraction equation of the six-equation two-phase model, with ρ_{I} representing an interface density. Similar to [3], this term is not included in the present multiphase model (1). The purpose of the term $\mathcal{M}/\rho_{\mathrm{I}}$ in [11] was to indicate the influence of the mass transfer process on the evolution of the volume fraction. Nonetheless, the rigorous derivation of the pressure-relaxed model (5) from the system (1) reveals that indeed mass transfer terms affect α_k via the pressure relaxation process, as we observe from the contribution of $\mathcal{M}$ appearing in (5a), (5b). Note that neglecting the term $\mathcal{M}/\rho_{\mathrm{I}}$ in the six-equation model of [11] does not affect the numerical model and the numerical results presented there, since $\nu = 0$ or $\nu \to \infty$, and the numerical procedure for treating instantaneous chemical relaxation consists in imposing directly algebraic thermodynamic equilibrium conditions.

3 Numerical Method

We focus now on the numerical approximation of the multiphase system (1), which we can write in compact vectorial form as

$$\partial_t q + \nabla \cdot \mathcal{F}(q) + \varsigma(q, \nabla q) = \psi_\mu(q) + \psi_\vartheta(q) + \psi_\nu(q) , \tag{10}$$

where $q = [\alpha_1, \alpha_3, \ldots, \alpha_N, \alpha_1\rho_1, \ldots, \alpha_N\rho_N, \rho\mathbf{u}, \alpha_1 E_1, \ldots, \alpha_N E_N]^{\mathrm{T}} \in \mathbb{R}^{3N-1+d}$ is the vector of the unknowns, $\mathcal{F}(q)$ represents the conservative portion of the system, and $\varsigma(q, \nabla q)$ is the non-conservative term. The source terms ψ_μ, ψ_ϑ, and ψ_ν in the system above contain mechanical, thermal, and chemical relaxation terms, respectively. To numerically solve the system (10), we use the same techniques that we have developed for the two-phase model in [11]. A fractional step method is employed, where we alternate between the solution of the homogeneous system

$\partial_t q + \nabla \cdot \mathcal{F}(q) + \varsigma(q, \nabla q) = 0$ and the solution of a sequence of systems of ordinary differential equations (ODEs) that take into account the relaxation source terms ψ_μ, ψ_ϑ, and ψ_ν. As in [11], the resulting method is mixture-energy-consistent, in the sense that (i) it guarantees conservation at the discrete level of the mixture total energy; (ii) it guarantees consistency by construction of the values of the relaxed states with the mixture pressure law. The method has been implemented by using the libraries of the CLAWPACK software [10].

3.1 Solution of the Homogeneous System

To solve the hyperbolic homogeneous portion of (10), we employ the wave propagation algorithms of [8, 9], which are a class of Godunov-type finite volume methods to approximate hyperbolic systems of partial differential equations. We shall consider here for simplicity the one-dimensional case in the x direction, and we refer the reader to [9] for a comprehensive presentation of these numerical schemes. We assume a grid with cells of uniform size Δx, and we denote with Q_i^n the approximate solution of the system at the ith cell and at time t^n, $i \in \mathbb{Z}$, $n \in \mathbb{N}$. The second-order wave propagation algorithm has the form

$$Q_i^{n+1} = Q_i^n - \frac{\Delta t}{\Delta x}(\mathcal{A}^+ \Delta Q_{i-1/2} + \mathcal{A}^- \Delta Q_{i+1/2}) - \frac{\Delta t}{\Delta x}(\tilde{F}_{i+1/2} - \tilde{F}_{i-1/2})\,. \quad (11)$$

Here $\mathcal{A}^\mp \Delta Q_{i+1/2}$ are the so-called fluctuations arising from Riemann problems at cell interfaces $(i + 1/2)$ between cells i and $(i + 1)$, and $\tilde{F}_{i+1/2}$ are correction terms for (formal) second-order accuracy. To define the fluctuations, a Riemann solver must be provided. For the present work, we have developed a numerical scheme in one and two spatial dimensions for the three-phase case, $N = 3$, by adopting a HLLC-type Riemann solver analogous to the one that we have presented in [11] for the two-phase case. This solver guarantees conservation of the partial densities $\alpha_k \rho_k$, the mixture momentum $\rho\mathbf{u}$, and the mixture total energy $E = \sum_{k=1}^{N} \alpha_k E_k$. This simple HLLC-type solver omits the discretization of the non-conservative terms Υ_k in the phasic energy equations. We refer to [11] for a discussion on this point and the rationale for this approach. We just remark here that for the two-phase case we have done comparisons of this HLLC-type solver with Riemann solvers that take into account the non-conservative terms Υ_k, including a Roe-type solver [11, 12] and a new Suliciu-type solver [1], and no relevant differences were observed in the results. Details on the Suliciu-type solver will be reported elsewhere.

3.2 Relaxation Steps

Similar to [7, 11], the numerical relaxation procedures to handle infinitely fast transfer processes are based on the idea of imposing directly equilibrium conditions to obtain a simple system of algebraic equations to be solved in each relaxation sub-step.

3.2.1 Mechanical Relaxation

We consider the solution of the system $\partial_t q = \psi_\mu(q)$ in the limit $\mu_{kj} \equiv \mu \to \infty$. We denote with superscript 0 the quantities at initial time, which come from the solution of the homogeneous system, and with superscript $*$ the quantities at final time, which are the quantities at mechanical equilibrium. First, we easily see that the exact solution of the system of ODEs gives $(\alpha_k \rho_k)^* = (\alpha_k \rho_k)^0$, $k = 1, \ldots, N$, and $(\rho \mathbf{u})^* = (\rho \mathbf{u})^0$, $E^* = E^0$, hence $\mathbf{u}^* = \mathbf{u}^0$ and $\mathcal{E}^* = \mathcal{E}^0$. We then integrate the equations for the phasic total energies by approximating the interface pressures $p_{\mathrm{I}kj}$ with their values at equilibrium $p^*_{\mathrm{I}kj} = p^*$. This gives N equations of the form

$$(\alpha_k E_k)^* - (\alpha_k E_k)^0 = (\alpha_k \mathcal{E}_k)^* - (\alpha_k \mathcal{E}_k)^0 = -p^*(\alpha_k^* - \alpha_k^0), \quad k = 1, 2, \ldots, N\,. \tag{12}$$

Imposing the pressure equilibrium conditions $p_k = p^*$, $\forall k = 1, \ldots, N$, at final time the phasic internal energies are then expressed as $\mathcal{E}_k^* = \mathcal{E}_k(p^*, (\alpha_k \rho_k)^0/\alpha_k^*)$. With these relations, system (12) and the constraint $\sum_{k=1}^{N} \alpha_k = 1$ give $N + 1$ equations for the unknowns α_k^*, $k = 1, \ldots, N$, and p^*. For the particular case of the SG EOS, the problem can be reduced to the solution of a polynomial equation of degree N for the equilibrium pressure p^*. Furthermore, for the case studied here with three phases, $N = 3$, and two gaseous phases governed by a SG EOS with $\varpi_k = 0$ (see Eq. (3)), the polynomial equation of degree 3 for p^* reduces to a quadratic equation, whose physically admissible solution is easily found.

3.2.2 Thermal Relaxation

If thermal relaxation terms are also activated, then we consider the solution of a system of the form $\partial_t q = \psi_\mu(q) + \psi_\vartheta(q)$, with $\mu_{kj} \equiv \mu \to \infty$ for all phase pairs, and $\vartheta_{kj} \equiv \vartheta \to \infty$ for some desired pairs (k, j). Let us assume instantaneous thermal equilibrium for M phases, $2 \le M \le N$, in addition to mechanical equilibrium for all phases. We will denote equilibrium values with the superscript $**$. Then, similar to the case of pressure relaxation, we can write $(\alpha_k \rho_k)^{**} = (\alpha_k \rho_k)^0$, $k = 1, \ldots, N$, $(\rho \mathbf{u})^{**} = (\rho \mathbf{u})^0$, $E^{**} = E^0$, and $\mathcal{E}^{**} = \mathcal{E}^0$. Moreover, we write $N - M$ equations of the form (12) with $(\cdot)^0$ replaced by $(\cdot)^*$ and $(\cdot)^*$ replaced by $(\cdot)^{**}$, the mechanical equilibrium conditions $p_k^{**} = p^{**}$, $\forall k = 1, \ldots, N$, and the thermal equilibrium conditions $T_k^{**} = T^{**}$ for M phases. All these relations give a system of algebraic equations to be solved for the equilibrium values α_k^{**}, p^{**}. As for the mechanical relaxation step, the solution of this system of algebraic equations can be reduced to the solution of a polynomial equation of degree N for the pressure p^{**} when the SG EOS is adopted. The problem reduces further to the solution of a quadratic equation for the case $N = 3$ with two gaseous phases governed by SG pressure laws with $\varpi_k = 0$.

3.2.3 Thermo-Chemical Relaxation

If thermo-chemical relaxation is activated for the species that may undergo liquid–vapor transition, then we need to solve a system of ODEs of the form $\partial_t q = \psi_\mu(q) + \psi_\vartheta(q) + \psi_\nu(q)$, with $\mu_{kj} \equiv \mu \to \infty$ for all phase pairs, $\vartheta_{kj} \equiv \vartheta \to \infty$ for some phase pairs (k, j), and $\nu \to +\infty$ for the phase pair $(1, 2)$. Let us assume instantaneous thermal equilibrium for M phases, including at least the phases 1 and 2. We denote the quantities at thermodynamic equilibrium with the superscript $\oplus$. First, we can write $\rho^\oplus = \rho^0$, $(\rho\mathbf{u})^\oplus = (\rho\mathbf{u})^0$, $E^\oplus = E^0$, and $\mathcal{E}^\oplus = \mathcal{E}^0$. Moreover, we write $N - M$ equations of the form (12) with $(\cdot)^0$ replaced by $(\cdot)^{**}$ and $(\cdot)^*$ replaced by $(\cdot)^\oplus$, the mechanical equilibrium conditions $p_k^\oplus = p^\oplus$, $\forall k = 1, \dots, N$, the thermal equilibrium conditions $T_k^\oplus = T^\oplus$ for M phases, and the chemical equilibrium condition $g_1^\oplus = g_2^\oplus$. This set of algebraic equations can be solved for the values of the equilibrium pressure $p^\oplus$, the equilibrium volume fractions $\alpha_k^\oplus$, and the equilibrium densities $\rho_k^\oplus$. For the case of the SG EOS considered here, we use a solution procedure similar to the two-phase case [11]. First, we reduce the set of algebraic conditions excluding the chemical equilibrium relation to the solution of a quadratic equation for the temperature as a function of the equilibrium pressure, $T^\oplus = T^\oplus(p^\oplus)$. Then, the expression of $T^\oplus(p^\oplus)$ is introduced into the equilibrium condition $g_1^\oplus = g_2^\oplus$. This gives an equation for $p^\oplus$, which is solved by Newton's iterative method.

4 Numerical Experiments

We now present some numerical experiments for three-phase flows involving the liquid and vapor phases of water and a third non-condensable phase. The parameters of the SG EOS for water are those used in [11] (we use hereafter the subscripts l and v for liquid and vapor, respectively): $\gamma_\mathrm{l} = 2.35$, $\gamma_\mathrm{v} = 1.43$, $\eta_\mathrm{l} = -1167 \times 10^3$ J/kg, $\eta_\mathrm{v} = 2030 \times 10^3$ J/kg, $\varpi_\mathrm{l} = 10^9$ Pa, $\varpi_\mathrm{v} = 0$ Pa, $\kappa_{v\mathrm{l}} = 1816$ J/(Kg $\cdot$ K), $\kappa_{v\mathrm{v}} = 1040$ J/(Kg $\cdot$ K), $\eta'_\mathrm{l} = 0$ J/(Kg $\cdot$ K), $\eta'_\mathrm{v} = -23.4 \times 10^3$ J/(Kg $\cdot$ K).

4.1 Three-Phase Water Cavitation Tube

We perform a test that is similar to the two-phase cavitation tube experiment presented in [11, 14]. We consider a tube filled initially with liquid water with a uniformly distributed small amount of water vapor $\alpha_{\mathrm{wv}} = 10^{-2}$ and a small amount of air (non-condensable gas) $\alpha_{\mathrm{g}} = 10^{-1}$. Air is modeled as an ideal gas with $\gamma_{\mathrm{g}} = 1.4$ ($\eta_{\mathrm{g}} = 0$ J/kg, $\varpi_{\mathrm{g}} = 0$ Pa). The initial pressure is $p_0 = 10^5$ Pa, and the initial densities correspond to the temperature $T_0 = 354$ K. A velocity discontinuity is set at the initial time at the middle of the tube, with $u_0 = -20$ m/s on the left and $u_0 = 20$ m/s on the right. We use 3000 grid cells over the interval [0, 1], and CFL = 0.5. We perform the simulation with different levels of activation of instantaneous relaxation processes: (i) only mechanical relaxation (p-relaxation); (ii) mechanical relaxation for all the three phases and thermal relaxation for the liquid–vapor pair only (pT(lv)-relaxation); (iii) mechanical and thermal relaxation for all the phases (pT-relaxation); (iv) mechanical relaxation for all the phases and thermal and chemical relaxation for the liquid-vapor pair (pT(lv)g-relaxation); (v) mechanical and thermal relaxation for all the phases and chemical relaxation for the liquid-vapor pair (pTg-relaxation). Second-order results are displayed in Fig. 1 for the pressure, the velocity, the total gaseous volume fraction $\alpha_{\mathrm{wv}} + \alpha_{\mathrm{g}}$, and the vapor mass fraction. In all the cases, we observe two rarefactions propagating in opposite directions that produce a pressure decrease in the middle region of the tube, and, correspondingly, an increase of the total gaseous component. For the cases with activation of mass transfer, i.e., pT(lv)g- and pTg-relaxation, two evaporation waves develop, causing an increase of the vapor mass fraction in the middle region. Note that in these cases the pressure decreases in the cavitation zone until the saturation value is reached, whereas the pressure reaches much lower values here if mass transfer is not activated. By inspecting the results, we observe that the speed of the leading edges of the two rarefactions decreases for any additional instantaneous thermal equilibrium process that we activate in the computation, consistently with the sub-characteristic property demonstrated theoretically for the hierarchy of relaxed models in Sect. 2.1. Let us note that chemical relaxation is not active here around the rarefaction fronts since mass transfer in this test is activated under the metastability condition $T_{\mathrm{liquid}} > T_{\mathrm{sat}}(p)$.

4.2 Underwater Explosion Close to a Rigid Surface

In this test, we simulate a cylindrical underwater explosion (UNDEX) close to a rigid surface. Following [15], we consider an initial bubble of highly pressurized gas (combustion products) surrounded by liquid water and located near an upper flat wall. Three fluid components are involved in this problem: liquid water, water vapor, and combustion gases. The domain is $[-0.6, 0.6] \times [-0.7, 0]\,\mathrm{m}^2$, and the bubble initially is located at $(x_{\mathrm{b}}, y_{\mathrm{b}}) = (0, -0.22)$ m, and it has radius $r_{\mathrm{b}} = 0.05$ m. Inside the bubble, we set initially a pressure $p = 8290 \times 10^5$ Pa, a gas density $\rho_{\mathrm{g}} = 1400\,\mathrm{kg/m}^3$, and volume fractions $\alpha_{\mathrm{wl}} = \alpha_{\mathrm{wv}} = 10^{-8}$ for the water phases. Outside the bubble, we set $p = 10^5$ Pa, $T = 303$ K, and the volume fractions $\alpha_{\mathrm{wv}} = 10^{-4}$ and $\alpha_{\mathrm{g}} = 10^{-7}$, for water vapor and gas, respectively. An ideal gas law is used for the combustion gases, with $\gamma_{\mathrm{g}} = 2$. In this test, thermal and chemical relaxation are activated for the liquid–vapor water pair only. This explosion problem is characterized by a complex

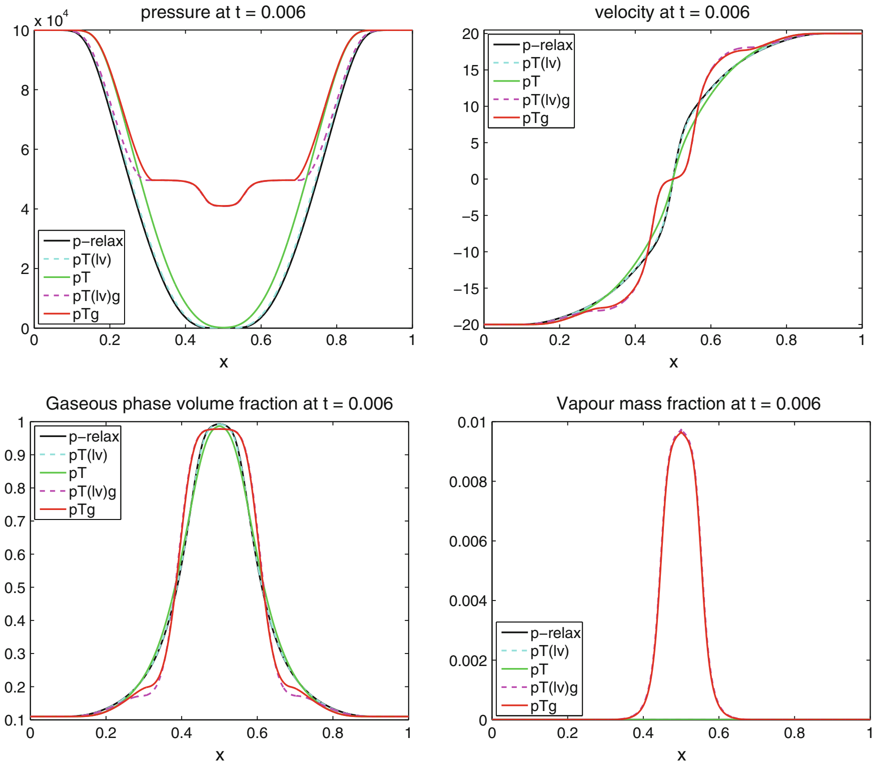

Fig. 1 Numerical results for the pressure, velocity, total gas volume fraction, and vapor mass fraction for the water cavitation tube test

pattern of shocks and rarefaction waves [15], and the likely occurrence of creation and collapse of vapor cavities in the liquid region close to the wall, due to the strong rarefactions and subsequent recompression. We show in Fig. 2 pseudo-color plots of the pressure at two different times. At $t = 0.2$ ms (upper left plot), the circular shock created by the explosion has reflected from the wall; at time $t = 0.35$ ms (lower left plot), a low-pressure cavitation region has developed close to the surface. The pressure and water vapor mass fraction histories in time at the point $(0, 0)$ at the center of the wall are also displayed in the two plots on the right of Fig. 2. We clearly observe the pressure peak corresponding to the instant at which the circular shock hits the wall, the drop of the pressure and consequent growth of a vapor region in this zone, which eventually disappears due to the recompression at later times. In the literature, these type of UNDEX problems are typically simulated by simpler single-fluid models [15], or by two-phase flow models [2] that are only able to describe mechanical cavitation processes, that is growth/collapse of gas cavities due to pressure variations, with no liquid-vapor transition. In contrast, our three-phase

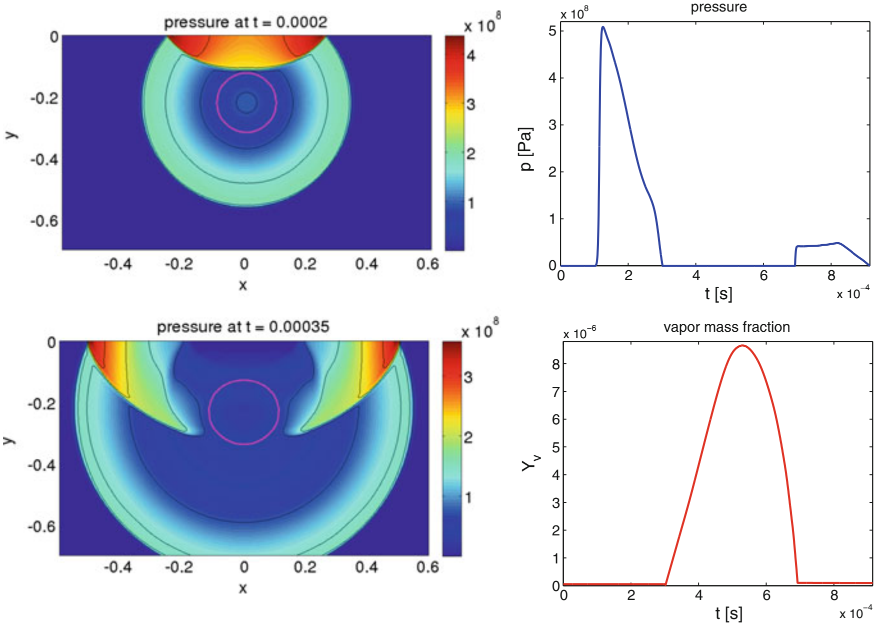

Fig. 2 Numerical results for the UNDEX experiment. Left: pressure field at time $t = 0.2\,\text{ms}$ (top) and $t = 0.35\,\text{ms}$ (bottom). The thick solid circle line indicates the water/bubble interface. Right: pressure history (top) and vapor mass fraction history (bottom) at the point $(0, 0)$ at the center of the wall

flow model allows a more accurate description of the thermodynamics of cavitation processes, which involve liquid–vapor phase change.

5 Conclusions

We have presented a numerical model for multiphase compressible flows involving the liquid and vapor phases of one species and a third inert gaseous phase. The model includes mechanical, thermal, and chemical relaxation processes. The multiphase equations are solved by a mixture-energy-consistent finite volume wave propagation method combined with simple and robust procedures for the stiff relaxation terms. Numerical results show the efficiency of the presented method in modeling complex wave patterns with thermal and mass transfer processes. An analytical study of the characteristic speeds of the hierarchy of relaxed models associated with the parent relaxation model has been also presented. The presented model is an extension of the two-phase flow model that we have introduced in [11]. This novel extension allows us the simulation of problems where the dynamical appearance of vapor cavities and evaporation fronts in a liquid is coupled to the dynamics of a third non-condensable gaseous component governed by its own equation of state. An example of application illustrated in the present work is the simulation of an underwater explosion close to a rigid wall, where highly pressurized combustion gases (non-condensable phase) trigger cavitation processes in a liquid. Another application example can be found in [13].

Acknowledgements The authors gratefully acknowledge support from the French DGA Grant N. 2012.60.0011.00.470.75.01 for M. Pelanti, the Norwegian RCN Grant N. 234126/E30 for M. Pelanti and T. Flåtten, the Taiwanese NSC Grant N. 99-2115-M-002-005-MY2 for K.-M. Shyue.

References

1. F. Bouchut, *Nonlinear Stability of Finite Volume Methods for Hyperbolic Conservation Laws, and Well-Balanced Schemes for Sources* (Birkhäuser, 2004)
2. A. Daramizadeh, M.R. Ansari, Numerical simulation of underwater explosion near air-water free surface using a five-equation reduced model. Ocean Eng. **110**, 25–35 (2015)
3. T. Flåtten, H. Lund, Relaxation two-phase models and the subcharacteristic condition. Math. Models Methods Appl. Sci. **21**, 2379–2407 (2011)
4. T. Flåtten, A. Morin, S.T. Munkejord, Wave propagation in multicomponent flow models. SIAM J. Appl. Math. **8**, 2861–2882 (2010)
5. A.K. Kapila, R. Menikoff, J.B. Bdzil, S.F. Son, D.S. Stewart, Two-phase modeling of deflagration-to-detonation transition in granular materials: reduced equations. Phys. Fluids **13**, 3002–3024 (2001)
6. O. Le Métayer, J. Massoni, R. Saurel, Elaborating equations of state of a liquid and its vapor for two-phase flow models. Int. J. Therm. Sci. **43**, 265–276 (2004)
7. O. Le Métayer, J. Massoni, R. Saurel, Dynamic relaxation processes in compressible multiphase flows. Application to evaporation phenomena. ESAIM Proc. **40**, 103–123 (2013)
8. R.J. LeVeque, Wave propagation algorithms for multi-dimensional hyperbolic systems. J. Comput. Phys. **131**, 327–353 (1997)
9. R.J. LeVeque, *Finite Volume Methods for Hyperbolic Problems* (Cambridge University Press, Cambridge, 2002)
10. LeVeque, R.J.: clawpack. http://www.clawpack.org
11. M. Pelanti, K.-M. Shyue, A mixture-energy-consistent six-equation two-phase numerical model for fluids with interfaces, cavitation and evaporation waves. J. Comput. Phys. **259**, 331–357 (2014)
12. M. Pelanti, K.-M. Shyue, A mixture-energy-consistent numerical approximation of a two-phase flow model for fluids with interfaces and cavitation, in *Hyperbolic Problems: Theory, Numerics, Applications, Proceedings of 14th International Conference on Hyperbolic Problems, AIMS* (2014), pp. 839–846
13. F. Petitpas, J. Massoni, R. Saurel, E. Lapebie, L. Munier, Diffuse interface models for high speed cavitating underwater systems. Int. J. Multiphase Flows **35**, 747–759 (2009)
14. R. Saurel, F. Petitpas, R. Abgrall, Modelling phase transition in metastable liquids: application to cavitating and flashing flows. J. Fluid Mech. **607**, 313–350 (2008)
15. W.F. Xie, T.G. Liu, B.C. Khoo, Application of a one-fluid model for large scale homogeneous unsteady cavitation: the modified Schmidt model. Comput. Fluids **35**, 1177–1192 (2006)